Chapter 9
Variation of Soot Structure Along the Exhaust Aftertreatment System—Impact of Oxygenated Diesel Blends on the Soot/Catalyst Interactions

Nahil Serhan

Abstract Particulate matter structural modifications do not only impact the oxidative/mutagenic properties of the particulates but also influence the motion and contact between the aggregates in the exhaust. Those interactions have a direct impact on the porosity, permeability, and packing density of the soot cake deposited in the diesel particulate filter (DPF). This in turn will influence the filtration efficiency and pressure drop in the DPF channels. Morphology of the PM combined with the carbon layer nanostructure also has a direct impact on the DPF regeneration capability. After recognizing the importance of the particulates' structure on the DPF performance, it becomes a subject of interest to understand if the engine-out PM will face any modifications within the aftertreatment units, e.g., diesel oxidation catalyst, selective catalytic reduction catalyst, etc., before being trapped in the DPF. While the dependency of the PM characteristics on its fueling source and engine technology is a well-researched topic, limited work has been carried out regarding the impact of the aftertreatment system on the structure (i.e., morphology and nanostructure) and chemical characteristics of the exhaust PM. This chapter will discuss the different theories and experimental work provided in the literature regarding the impact of aftertreatment systems on the PM characteristics. Special attention will be given on the impact of alcohols and other oxygenated fuels on this mechanism compared to conventional diesel fuel.

Keywords Alcohol · Soot · Particulate matter · DPF · DOC · SCR · Aftertreatment

N. Serhan (✉)
Wärtsilä Catalyst Systems R&D, Vaasa, Finland
e-mail: nahil.serhan@wartsila.com

A. P. Singh and A. K. Agarwal (eds.), *Novel Internal Combustion Engine Technologies for Performance Improvement and Emission Reduction*, Energy, Environment, and Sustainability, https://doi.org/10.1007/978-981-16-1582-5_9

9.1 Introduction

Diesel smoke, so-called particulate matter (PM), can be presented as a combination of carbonaceous material (soot) blended with several types of inorganic and organic substances, resulting in mutagenic and carcinogenic elements by nature (Silverman et al. 2012). Soot structural modifications (i.e., morphology) do not only impact the oxidative/mutagenic properties of the soot but also influence the motion and contact (i.e., convective or diffusive flow) between the particulates which in turn impacts the magnitude of the Peclet number (Pe) accordingly. Pe is a dimensionless factor whose magnitude strongly depends on the soot morphological aspects, mainly the primary particulate size (d_{p0}) and to a lesser extent, the radius of gyration (R_g) (Konstandopoulos et al. 2002). The lower the Pe (<1) the more open and porous the soot cake is (i.e., layer of soot deposited in the DPF channels) and the higher the Pe ($1 < Pe < 5$) the more compact it is. In general, an increase in d_{p0} will yield a higher Pe number and vice versa (Konstandopoulos et al. 2002). Factors as the soot-cake permeability, packing density, porosity, pressure drop in the channels and DPF thermal behavior during regeneration can be calculated (i.e., simulated) once obtaining the Pe number (Konstandopoulos et al. 2002; Chiatti et al. 2009; Konstandopoulos and Kostoglou 2004). The reader is referred to (Konstandopoulos et al. 2002; Chiatti et al. 2009; Konstandopoulos and Kostoglou 2004) for a more detailed interpretation of the incorporated formulas that link the Pe number with the soot-cake characteristics. As a matter of fact, recognizing the filtration efficiency of a DPF is important; however, predicting the exact dimensioning of the system to optimize the resulted backpressure is even more critical, especially in the norm of the severe legislations and economic viability of diesel-powered vehicles (Fig. 9.1).

After recognizing the importance of the particulates' structure on the DPF performance, it becomes a subject of interest to understand if the exhaust particulates will face any modifications within the aftertreatment units, e.g., diesel oxidation catalyst (DOC), selective catalytic reduction (SCR), etc., before being trapped in the DPF. While the dependency of the soot structure on its fuelling source and engine technology is a well-researched topic, to our knowledge, limited work (Ma et al. 2014;

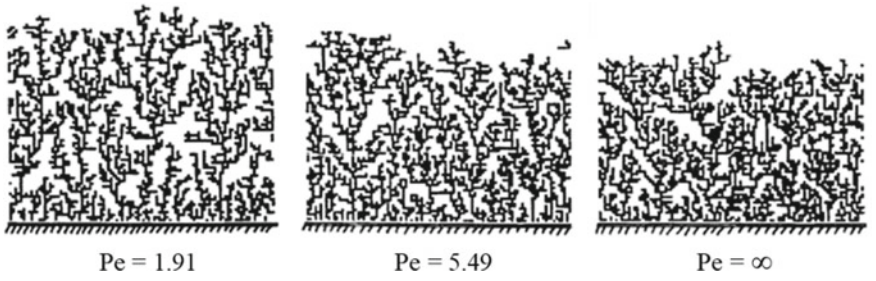

Fig. 9.1 Soot-cake representation with regard to its Peclet number. Reproduced from (Tassopoulos et al. 1989)

Liati et al. 2013; Lapuerta et al. 2007; Fayad et al. 2015; Lee and Zhu 2005; Serhan et al. 2019) has been carried out regarding the impact of the aftertreatment system on the structure of the exhaust PM (i.e., morphology and nanostructure). The chapter will be divided into two sections, research work based on (i) diesel oxidation catalyst and (ii) hydrocarbon-SCR (HC-SCR) catalyst. The impact of the fuel type will be discussed in each section separately.

9.2 Variation in Soot Structure Throughout DOC

Lapuerta et al. (2007) studied the impact of changing the soot sampling point in the exhaust line to check if d_{p0} will be altered by the thermal or fluid-dynamic conditions along the line. However, the study did not involve any aftertreatment unit. It was seen that d_{p0} remains constant throughout all the tested positions since as reported, the exhaust temperature level (110–324 °C) was not enough to launch any chemical reactions with the soot surface. Liati et al. (2013) studied the morphological and nanostructure aspects of soot particulates upstream and downstream the DOC in an effort to understand the impact of this catalyst on the particulate's oxidative reactivity. Concerning the morphological alterations, slight reduction was noted along d_{p0}- when the particulates flow throughout the catalyst. This was due to the devolatilization of the soluble/semi-volatile organic fraction from the particulates' surface; however, these changes were not linked with the existence of any possible carbon oxidation phenomenon. As for the graphitization order, slightly more ordered structure was presented downstream the DOC, and therefore, to some extent, the particulates were considered less reactive toward oxidation. Close edge X-ray absorption fine structure analysis (NEXAFS) was also employed to understand the difference in the particulate's surface functional compounds upstream and downstream the catalyst. It was shown that marginal changes took place downstream the DOC and more specifically, most of the carboxyl functionalities had disappeared and the soot seemed to be more homogeneous in its chemical structure. Ma et al. (2014) studied the impact of the DOC on the particulate's carbon layer arrangement and its corresponding oxidative reactivity. The analysis showed that DOC can alter the primary particulate's inner structure in a way that makes it more ordered toward graphitization, e.g., longer carbon layer length (L_a) and remarkably shorter interlayer spacing (d_{002}). As for the oxidative behavior, the post-catalyst soot seemed to be more reactive, yet a different oxidation mode was recorded compared to that in the pre-catalyst case. To be more specific, the soot mass loss was extremely faster than that of the pre-catalyst test at the early stages of the oxidation (before 50% soot mass loss); however, at later stages (after 50%), the oxidation rate turned to be slower and the residual ash mass significantly higher. Concerning the residuals, they were mainly influenced by the sample collection method and not by any direct soot interactions with the DOC. Longer period was needed to collect the soot downstream the catalyst since the increased concentrations of nitrogen dioxides (NO_2) (resulted from the nitrogen oxide (NO) oxidation in the DOC) continuously oxidized the soot placed on the filter. However,

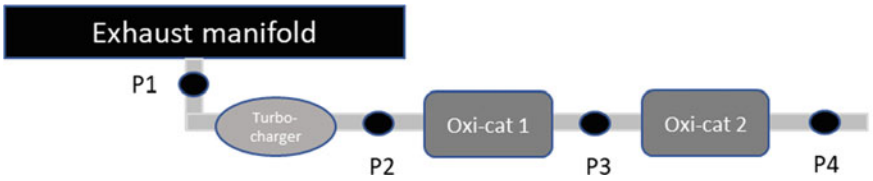

Fig. 9.2 Sampling collection positions for reference (Lee and Zhu 2004, 2005)—self-drawn by author

during the collection time, the ash deposition remained intact and did not oxidize, thus increasing the ash percentage of the sample placed after the DOC. The soot nanostructure variations were also recorded throughout the different stages of the temperature-controlled oxidation to further investigate the oxidation mechanism of the soot samples (pre- and post-catalyst). It was concluded that the soot collected upstream the DOC undergoes a surface burning process; in other words, it keeps a shell-core structure along all the oxidation period. As for the post-catalyst particulates, the same oxidation mode as that of the "biodiesel oxidation" (Song et al. 2006) was seen for this testing case. In summary, despite the more graphitic initial structure, the high-resolution transmission electron microscopy (HRTEM) analysis revealed that the soot undergoes an internal-burning process at the early stages of the oxidation which leads to a capsule-like structure. The significant energy released during this phase helps to thermally restructure the soot silhouette and transform it to a closed outer shell profile. The highly stable configuration of the latter is the main reason for the slower oxidation rates recorded after the first 50% of the soot weight loss. It was speculated that the DOC contributed to the devolatilization of the surface volatile compounds, which in turn generated this unique mode of oxidation. Lee and Zhu (Lee and Zhu 2004, 2005) studied the evolution of the soot morphological parameters along the different positions of the exhaust system (that includes two DOCs) as a function of engine speed and load condition. The different soot sampling positions are presented in Fig. 9.2. The analysis showed that independently from the engine operating settings, the first DOC helped to reduce the particulates R_g and d_{p0} and increased their circularity, e.g., higher fractal dimension (D_f). The reduction in d_{p0} was related to the existence of a soot catalytic oxidation, which was also confirmed through qualitative inspection for the HRTEM micrographs. It was shown that upstream the catalyst, the particulates presented the standard graphitic configuration of diesel soot where the primary particulates are mostly spherical and quite distinct from the other spherules. However, downstream the catalyst, the primary particulates appear to have no definite borders and seem to be fused in each other, indicating the presence of catalytic oxidation. The second DOC (Position P4) also reduces d_{p0}; however, the particulates R_g tend to slightly increase and their geometrical configuration highlights a more chain-like structure (lower D_f). It was expected that the resulted particulates undergo an enhanced aerodynamic mixing after going out of the catalyst (after 200 cm), which in turn favors their aggregation together to yield larger particulates with a more complex geometry. Overall, it was seen that

d_{p0} and R_g decrease progressively throughout the catalysts with R_g presenting a bigger drop compared to d_{p0}. It was speculated that this further reduction in R_g could possibly arise from the breakdown of the particulates throughout the catalyst channels along with reduction in the interstitial distances among the spherules. However, the average number of the primary particulates in the aggregates (n_{p0}) was not evaluated in this study, keeping those findings (i.e., breakdown and reduction in interstitial spacing) as theoretical approaches and not proved by analysis.

Fayad et al. (2015) investigated the influence of the DOC with regard to the oxidation/reduction mechanism of the soot particulates produced from the combustion of diesel, rapeseed methyl ester (RME), and butanol/RME/diesel blend. It was seen that DOC can help in reducing the small-scale particulates (<20 nm) by diffusion mechanism (trapping) and can also result on average with larger soot particulates because of an enhanced collision phenomenon in the catalyst channels. This theory was further verified by morphologically analyzing the particulates, upstream and downstream the catalyst. From the analysis, it was reported that after passing the DOC, the collected soot tended to present a greater n_{p0} and a larger R_g compared to these tested upstream the catalyst, independent of the fuel type. Oxygenated fuel combustion results in particulates which are characterized with smaller primary particles and more skeletal aggregates compared to the diesel case. This, in turn, makes the particles produced from oxygenated fuels more easily trapped in the DOC. However, DOC modified neither the particulates' d_{p0} nor the carbon layers' arrangements, highlighting that a longer soot/catalyst residence time was required to perform those alterations (soot oxidation).

9.3 Variation in Soot Structure Throughout HC-SCR

Serhan et al. (2019) investigated the impact of a silver alumina (Ag/Al_2O_3) HC-SCR catalyst on the morphology and nanostructure of the soot aggregates produced from the combustion of diesel and diesel/tri-propylene glycol ether (TPGME) blends (20% vol. basis, TP20). Numerous studies in the literature proved the advantageous effect of PGMEs in reducing the engine-out PM emissions, particularly TPGME which was recognized for yielding near non-sooting combustion (Burke et al. 2015; Natarajan 2001; González 2001). The catalyst role was evaluated upon three main areas, the exhaust temperature by varying engine load (2 and 4 bars indicated mean effective pressure (IMEP)), fuel type, and hydrogen (H_2) present in the exhaust. H_2 gas has been recognized as a promoter for the Ag/Al_2O_3 de-NOx activity, especially in the low-temperature regions when enough reductants are available (Breen et al. 2007; Theinnoi et al. 2008). This research work present in-depth detail on the catalyst and fuel-type impact on soot particles and will be detailed following two separate sections, the first highlights the impact on soot morphology and the second highlights the nanostructure modifications.

9.3.1 Catalyst Impact on the Morphology

9.3.1.1 Low Exhaust Temperature Condition

The different soot morphological parameters including R_g, n_{p0}, and D_f for the different testing conditions at low load operation (2 bar IMEP, 180 °C) are plotted in Fig. 9.3. Also, the normal distribution of the primary particulate's size (d_{p0}) is plotted in Figure.

It is seen that with or without the presence of H_2, aggregates with greater R_g and n_{p0} are seen after the catalyst for both, diesel and TP20 fueling. Therefore, it can be concluded that only a limited portion of the particulates have been trapped inside the catalyst, as it was suggested earlier in reference (Fayad et al. 2015). Besides, it is expected that upon passing the catalyst channels, the soot particulates have faced higher chances of collision with the other neighboring particulates and as a result more mature aggregates (i.e., by size) are spotted downstream the HC-SCR. Furthermore, more spherical particulates were seen downstream the catalyst as suggested from the higher D_f values recorded in Fig. 9.3. This could be also the result of the enhanced collision process suggested earlier. Furthermore, the oxidation/activation of the HCs (exothermic reactions) throughout the catalyst along with the localized thermal effect of the H_2 are likely to increase the local and overall temperature of the catalyst. Higher catalyst temperatures can also help in thermally restructuring the soot shape into a more spherical entity, especially when H_2 is presented. Although it can be assumed that a worsened DPF trapping efficiency has resulted from the presence of more compact and spherical aggregates, the remarkable increase in

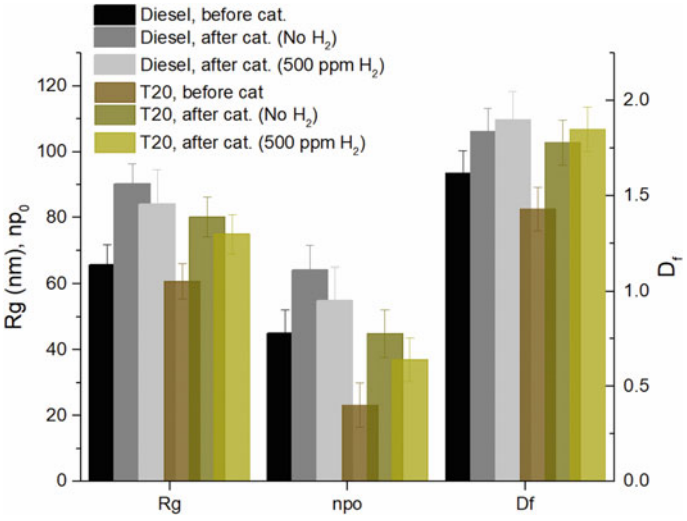

Fig. 9.3 Variation of D_f, n_{p0}, and R_g throughout the HC-SCR in the presence and absence of H_2 at 2 bar IMEP. Reproduced from (Serhan et al. 2019)

the overall particulate's size is expected to compensate their impact (Fayad et al. 2015). This assumption is mainly triggered from the fact the particulate's diffusion/convection pathway in a DPF (i.e., filtration mechanism) is most pronounced from the particulates' size and not their shape.

Concerning d_{p0}, insignificant variations were spotted in the absence of H_2 for both fueling conditions (Fig. 9.4). However, in the presence of H_2, d_{p0} dropped by 2.7% in case of diesel and 3.6% in case of TP20. The only possible theory to clarify these results is that despite the limited residence time of the particulates in the catalyst channels, soot oxidation reactions were launched once H_2 is injected. As for the increased reduction seen in case of TP20 with respect to diesel, it is expected to be the outcome from the enhanced oxidative potential of soot produced from the combustion of TP20 compared to that produced from the combustion of diesel, as reported earlier in Serhan et al. (2018). These possible oxidation reactions are mostly generated from the increased level of NO_2 throughout the catalyst channels (i.e., transition of NO into NO_2 before being converted to N_2 during H_2-SCR-assisted cycle, as it is advised by Breen et al. (2007)) since this oxidizer can launch the soot oxidation reactions in a temperature region as low as 200 °C (Ehrburger 2002). This assumption was partially approved by Houel et al. (Houel et al. 2007) who reported that in low-temperature window (200 °C to 350 °C), H_2 addition will not only enhance the Ag/Al_2O_3 de-NOx activity but also withstand it. The simplified reaction pathways presenting the NO_2-soot-assisted oxidation mechanism are presented below:

$$C(s) + NO_2 \rightarrow CO + NO$$

$$C(s) + 2NO_2 \rightarrow CO_2 + NO$$

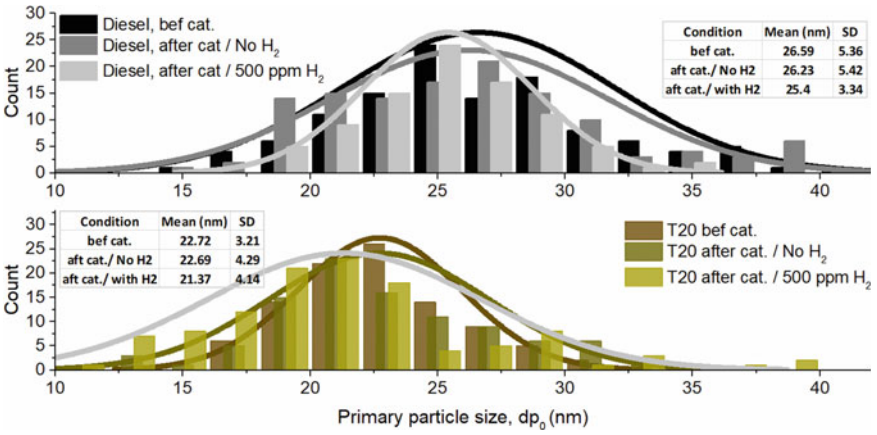

Fig. 9.4 Variation of d_{p0} throughout the HC-SCR in the presence and absence of H_2 at 2 bar IMEP. Reproduced from (Serhan et al. 2019)

Conversely, it is expected that O_2 should not assist the oxidation kinetics in this temperature window since higher temperature level (ranging in 500 to 700 °C) is needed. Furthermore, it is also confirmed in the literature that introducing H_2 gas in conjunction of an oxygen-rich flow (as the diesel exhaust) can change the Ag particulate chemistry to act as an oxidation catalytic agent. This is believed to result from the production of numerous sub-oxide elements (Kim et al. 2013) along with promoting the development of the active O_2- ions that can also assist the soot oxidation process (Vassallo et al. 1995).

In summary, it can be concluded that despite the low catalyst temperature (180 °C), the increase in the local NO_2 and surface O_2 functional species due to H_2 presence can partially oxidize the soot passing throughout the catalyst despite the very limited soot/catalyst residence time (flow-through substrate).

9.3.1.2 Medium Exhaust Temperature Condition

Similar to the earlier section, the same data type has been plotted in 5 and 6 after increasing the engine load to 4 bar IMEP and, respectively, the catalyst temperature to 280 °C (Figs. 9.5 and 9.6).

It is seen that the particulates surviving the catalytic reactions present greater R_g, n_{p0}, and D_f while d_{p0} is kept constant for the diesel case with insignificant drop seen only for the TP20 case. As a result, it is expected that the particulates have survived an enhanced aggregation mechanism throughout the catalyst channels and no possible catalytic oxidation is presented, even though that the catalyst temperature is increased by 100 °C compared to the 2 bar IMEP test. Introducing 500 ppm of H_2 activates the catalyst/soot synergies with significant modifications spotted compared to the 2 bar IMEP testing. As for diesel, a drop of 22% is seen for n_{p0}, 5.29% for d_{p0} and a total reduction of 10.16% for R_g. The significant reduction seen along d_{p0} confirms that with a little increase in the exhaust temperature, which is still representative

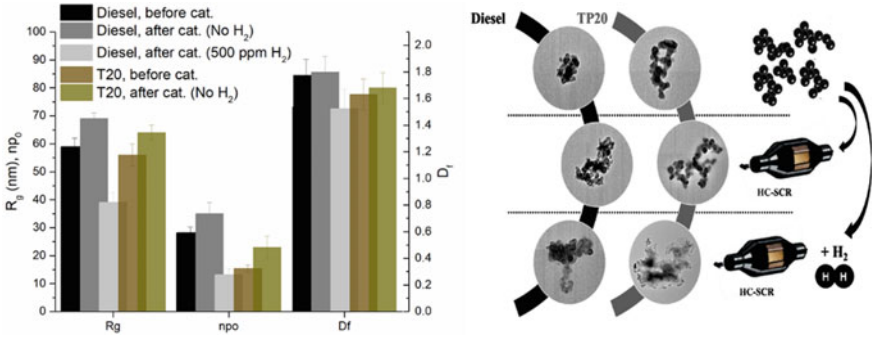

Fig. 9.5 Variation of D_f, n_{p0}, and R_g throughout the HC-SCR in the presence and absence of H_2 at 4 bar IMEP along with the representative HRTEM micrographs. Reproduced from (Serhan et al. 2019)

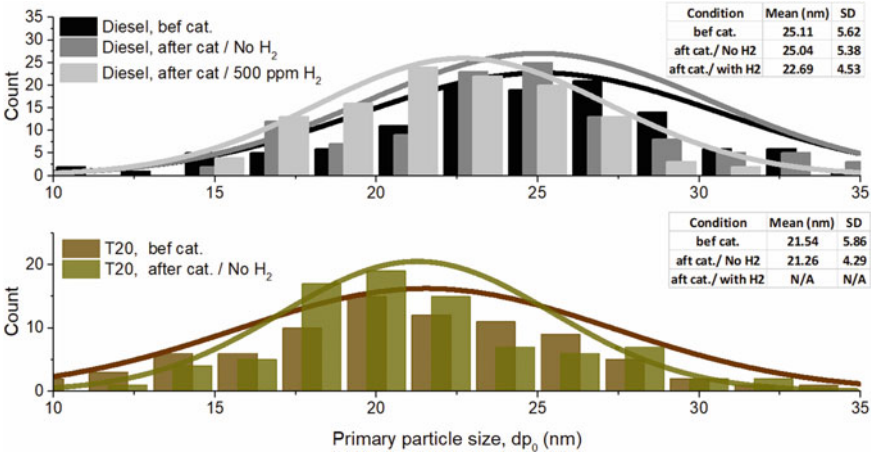

Fig. 9.6 Variation of d_{p0} throughout the HC-SCR in the presence and absence of H_2 at 4 bar IMEP. Reproduced from (Serhan et al. 2019)

of the low-temperature window, minute concentrations of H_2 can yield a powerful oxidation along the soot passing throughout the catalyst channels. It is expected that the NO_2-soot oxidation path is fully activated in this operating margin (~295 °C) and that the localized thermal impact of H_2 can also activate the O_2-soot oxidation pathway (Ehrburger 2002; Theinnoi et al. 2012). As for *Rg*, the catalyst impact was more pronounced with more severe reduction seen along this parameter compared to d_{p0}. A hypothesis could be drawn regarding this trend and can be mainly identified with two different approaches (Lee and Zhu 2004):

(a) Breakdown of the aggregates throughout the catalyst channels.
(b) Reduction in the interstitial distances among the primary particulates constituting the aggregates.

As n_{p0} also faces a noticeable drop downstream the catalyst, it is most probable that hypothesis (a) is the most dominant mechanism leading to this significant reduction in R_g. In addition, it is also speculated that the active oxygen species produced on the Ag particulates can also improve the soot/oxidizers contact and create electronic interaction between the surface of the catalyst and the soot particulates (thus promoting the breakdown phenomena). Concerning the soot fractal like particulates with more chain-like structure (~12% drop in D_f) are spotted downstream the catalyst. This configuration further indicates that hypothesis (b) is not valid for our analysis and highlights that a better DPF functionality can be expected with the application of the H_2-assisted HC-SCR catalyst to the exhaust flow. On the other hand, the increased local and global temperature of the catalyst is expected to thermally restructure the particulates into a more spherical entity (higher D_f). However, this was not the case with this testing condition, which in turn signifies that the catalytic oxidation reactions were remarkably prevailing at this slightly higher exhaust temperature and were

sufficiently energetic to dominate the thermal impact of the catalyst (i.e., resulting in more spherical-like particulates).

The catalytic oxidation of the soot was not only seen through the reduction in their d_{p0}, but also through qualitative inspection for the TEM micrographs (Fig. 9.5). It is seen that upstream the catalyst, the particulates collected present the standard graphitic configuration of a diesel soot, where the primary particulates are mostly spherical and quite distinct from the other spherules. However, downstream the catalyst, the primary particulates appear to have no definite borders and seem to be fused in each other, confirming the presence of a catalytic oxidation. This blur appearance is mostly seen in case of TP20 where no statistically significant number of particles were spotted on the TEM grids to produce a confident morphological analysis.

9.3.1.3 Catalyst Impact on Nanostructure

Since the soot morphological analysis highlights the presence of possible oxidation mechanism, it is of interest to check if any variation will be seen in the particulates' nanoscale arrangement. Such kind of information will be valuable to predict the reactivity of the aggregates surviving the catalytic reactions and can also give better insights to validate the oxidation reactions speculated from the reduction seen in d_{p0}. As no noticeable changes were seen with d_{p0} when H_2 is not introduced to the flow, the below analysis will account for the impact of the catalyst only in presence of the H_2. To simplify the results, Figure summarizes the resulted nanostructure parameters as a ratio of the values recorded upstream the catalyst compared to that seen downstream the catalyst (i.e., referred as post/pre in Fig. 9.7).

Concerning the low exhaust temperature condition (2 bar IMEP), similar trend was seen between diesel and TP20: the catalyst helps in reducing the length of the carbon layers (-8.5% L_a for diesel and -13% L_a for TP20) and further twist

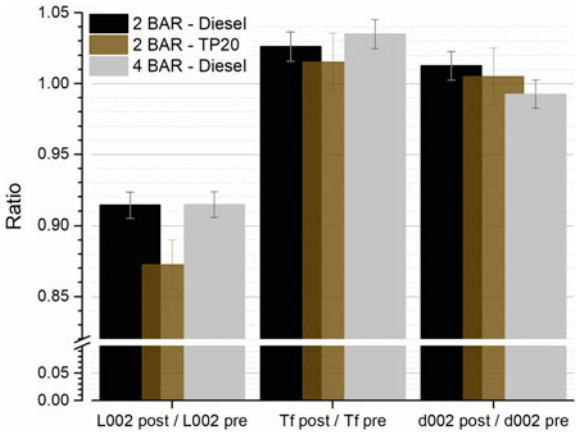

Fig. 9.7 Nanostructure parameter ratios including L_a, T_f, and d_{002}. Reproduced from (Serhan et al. 2019)

their skeleton (+2.8% T_f for diesel and +1.5% T_f for TP20). However, inconspicuous variation ranging within the data-error bars is seen along the interlayer spacing ($d_{002\ \text{after catalyst}}/d_{002\ \text{before catalyst}} \sim 1$) for both fueling. All the resulted parameters highlight a better oxidative reactivity for the particulates collected downstream the catalyst.

As for the medium exhaust temperature condition (4 bar IMEP), only diesel particulate will be evaluated since as discussed in the earlier section, no statistically significant number of soot aggregates survived the catalytic reactions in case of TP20. Starting with L_a, similar results are seen compared to the 2 bar IMEP condition while T_f show a further increase reaching 3.5%. However, d_{002} present a small drop of 1% compared to the pre-catalyst case, highlighting that more graphitic particulates are presented. It is expected that at this relatively higher exhaust temperature (~300 °C) the higher HC oxidation phenomena and increased NO_2-soot oxidation reactions can help in thermally restructuring the neighboring carbon layers into more ordered series, resulting in slightly more graphitic configuration (Ma et al. 2014). However, accounting all the nanostructure parameters, it can be speculated that despite this shorter interlayer spacing, the particulates are expected to be more reactive since the layers' curvature has been increased by 3.5% and L_a reduced by 8.5%. Carbon layer curvatures and length have been earlier proved to be more influential in dictating the particulate's reactivity compared to d_{002}, as reported in (Serhan et al. 2018).

Furthermore, to relate the nanostructure alterations to the possible soot/catalyst oxidation mechanism, the rate of soot burn-off in the catalyst will be calculated according to the difference in d_{p0} before and after the catalyst. Song et al. (2006) reported that during the first 40% stage of the soot burn-off cycle, the oxidation reactions should follow the surface burning mode mechanism. As a result, the following formula from reference (Song et al. 2006) can be used to assess the soot burn-off rate:

$$dp0\text{post SCR} \big/ dp0\text{pre SCR} = (1 + \text{z})^{1/3}$$

where z is the burn-off rate.

As a result, the soot burn-off is estimated to 8% in case of diesel and 10% in case of TP20 at 2 bar IMEP. Increasing the load to 4 bar IMEP increases the soot burn-off rate to 15% in diesel case while for TP20 there was no clear structure for the soot to measure the morphology/nanostructure parameters; however, it is expected to be higher than diesel case as it is in the 2 bar IMEP condition.

According to Song et al. (2006), surface burning mode mechanism is generally defined with slow combustion reactions translated with a notable reduction in L_a and no more than 3% increase in the particulate graphitic ordering (using Raman analysis) during the first 20% burn-off phase. However, Ma et al. (2014) presented a more detailed approach concerning the above. The study covers the progress of the soot nanostructure alterations during the oxidation process of separate particulates collected upstream and downstream a DOC catalyst. Different trends were seen along L_a and d_{002} between both samples, thus no clear conclusion can be beneficial for our

analysis; however, it was confirmed that T_f should increase by ~2% during the first 20% burn-off phase, independently from the soot collection point (downstream or upstream the DOC). Summarizing the findings of reference (Song et al. 2006) and (Ma et al. 2014), during the 20% burn-off phase, L_a is expected to decrease, while T_f is expected to slightly increase with moderate variation along d_{002}. Those findings positively correlate with the nanostructure variation shown in the analysis, thus confirming that these alterations are resulted from an enhanced oxidation mechanism in the catalyst channels.

9.4 Summary

This chapter focuses on the impact of the aftertreatment system on the soot aggregates regarding their morphology and nanostructure characteristics. The particulate trapping efficiency in DOC is linked to the parent fuel type. Oxygenated fuel combustion, e.g., butanol/RME/diesel blends, results in particulates which are characterized with smaller primary particles and more skeletal aggregates compared to the diesel case. This, in turn, makes the particles produced more easily trapped in the DOC. Also, it was seen that independent of the fuel type or exhaust temperature condition, soot particulates tend to aggregate with the other neighboring particulates leading to larger and more circular particulates downstream the DOC. The same hypothesis can be also drawn in case of HC-SCR when H_2 is not introduced upstream the catalyst. However, injecting minute concentration of H_2 helps in significantly modifying the morphology of the particulates which seem to be more dependent on the exhaust temperature when H_2 is presented. At low exhaust temperature (180 °C), particulates' aggregation remains the most dominant mechanism; however, it was seen that the soot primary particle diameter faces some reduction, highlighting the presence of oxidation reactions throughout the catalyst. Increasing the catalyst temperature (290°C) enhances the catalytical modification of the aggregates. It was seen that not only d_{p0} was reduced but also the soot radius of gyration and number of primary particles included in soot aggregates. Those alterations highlight that at this relatively higher exhaust temperature, soot particulates are not only oxidized, but they also tend to breakdown throughout the catalyst channels instead of being aggregated together. This impact was ameliorated when oxygenated diesel blend (TP20) was used. This is mainly due to the higher oxidative reactivity toward oxygen of the particulates produced from TP20 compared to neat diesel. The TP20 soot catalytic oxidation can be qualitatively inspected from the TEM micrographs. It is seen that upstream the catalyst, the particulates collected present the standard graphitic configuration of a soot particle, where the primary particulates are mostly spherical and quite distinct from the other spherules. However, after passing through catalyst, the primary particulates appear to have no definite borders and seem to be fused in each other, confirming the presence of strong catalytic oxidation in case of TP20 despite the limited residence provided throughout the catalyst channels.

References

Breen J et al (2007) A fast transient kinetic study of the effect of H2 on the selective catalytic reduction of NOx with octane using isotopically labelled 15NO. J Catal 246(1):1–9. https://doi.org/10.1016/j.jcat.2006.11.017

Burke U, Pitz WJ, Curran HJ (2015) Experimental and kinetic modeling study of the shock tube ignition of a large oxygenated fuel: tri-propylene glycol mono-methyl ether. Combus Flame 162(7):2916–2927. https://doi.org/10.1016/j.combustflame.2015.03.012

Chiatti G, Chiavola O, Falcucci G (2009) Soot morphology effects on DPF performance. SAE technical paper, 2009-01-1279

Ehrburger P et al (2002) Reactivity of soot with nitrogen oxides in exhaust stream. SAE Technical Paper, 2002-01-1683. https://doi.org/10.4271/2002-01-1683

Fayad MA et al (2015) Role of alternative fuels on particulate matter (PM) characteristics and influence of the diesel oxidation catalyst. Environ Sci Technol 49(19):11967–11973. https://doi.org/10.1021/acs.est.5b02447

González MA et al (2001) Oxygenates screening for advanced petroleum-based diesel fuels part 2: The effect of oxygenate blending compounds on exhaust emission. SAE Technical Paper, 2001-01-3632. https://doi.org/10.4271/2001-01-3632

Houel V et al (2007) Promoting functions of H2 in diesel-SCR over silver catalysts. Appl Catalysis B: Environ 77(1–2):29–34. https://doi.org/10.1016/j.apcatb.2007.07.003

Kim PS et al (2013) Effect of H2 on deNOx performance of HC-SCR over Ag/Al2O3: morphological, chemical, and kinetic changes. J Catalysis 301:65–76. https://doi.org/10.1016/j.jcat.2013.01.026

Konstandopoulos AG, Kostoglou M (2004) Microstructural aspects of soot oxidation in diesel particulate filters. SAE Technical Paper, 2004-01-0693. https://doi.org/10.4271/2004-01-0693

Konstandopoulos AG, Skaperdas E, Masoudi M (2002) Microstructural properties of soot deposits in diesel particulate traps. SAE Technical Paper, 2002-01-1015. https://doi.org/10.4271/2002-01-1015

Lapuerta M, Martos FJ, Herreros JM (2007) Effect of engine operating conditions on the size of primary particles composing diesel soot agglomerates. J Aerosol Sci 38(4):455–466. https://doi.org/10.1016/j.jaerosci.2007.02.001

Lee KO, Zhu J (2004) Evolution in size and morphology of diesel particulates along the exhaust system. SAE Technical Paper, 2004-01-1981. https://doi.org/10.4271/2004-01-1981

Lee KO, Zhu J (2005) Effects of exhaust system components on particulate morphology in a light-duty diesel engine. SAE Technical Paper, 2005-01-0184. https://doi.org/10.4271/2005-01-0184

Liati A et al (2013) Variations in diesel soot reactivity along the exhaust after-treatment system, based on the morphology and nanostructure of primary soot particles. Combus Flame 160(3):671–681. https://doi.org/10.1016/j.combustflame.2012.10.024

Ma Z et al (2014) Effects of diesel oxidation catalyst on nanostructure and reactivity of diesel soot. Energy Fuels 28:4376–4382. https://doi.org/10.1021/ef500467a

Natarajan M et al (2001) Oxygenates for advanced petroleum-based diesel fuels: Part 1. Screening and selection methodology for the oxygenates. SAE Technical Paper, 2001-01-3631. https://doi.org/10.4271/2001-01-3631

Serhan N, Tsolakis A, Martos FJB (2018) Effect of propylene glycol ether fuelling on the different physico-chemical properties of the emitted particulate matters: Implications of the soot reactivity. Fuel 219:1–11. https://doi.org/10.1016/j.fuel.2018.01.065

Serhan N et al (2019) Modifying catalytically the soot morphology and nanostructure in dieselexhaust: Influence of silver De-NOx catalyst (Ag/Al2O3). Appl Catalysis B: Environ 241:471–482

Silverman DT et al (2012) The diesel exhaust in miners study: a nested case-control study of lung cancer and diesel exhaust. J Natl Cancer Inst 104(11):855–868. https://doi.org/10.1093/jnci/djs034

Song J et al (2006) Examination of the oxidation behavior of biodiesel soot. Combust Flame 146(4):589–604. https://doi.org/10.1016/j.combustflame.2006.06.010

Tassopoulos M, O'Brien JA, Rosner DE (1989) Simulation of microstructure/mechanism relationships in particle deposition. Amer Inst Chem Eng J 35(6):967–980. https://doi.org/10.1002/aic.690350610

Theinnoi K et al (2008) Hydrogen promotion of low-temperature passive hydrocarbon-selective catalytic reduction (SCR) over a silver catalyst. Energy Fuels 22:4109–4114. https://doi.org/10.1021/ef8004515

Theinnoi K et al (2012) Diesel particulate filter regeneration strategies: Study of hydrogen addition on biodiesel fuelled engines. Energy Fuels 26(2):1192–1201. https://doi.org/10.1021/ef201355b

Vassallo J, Miró E, Petunchi J (1995) On the role of gas-phase reactions in the mechanism of the selective reduction of NOx. Appl Catalysis B: Environ 7:65–78. https://doi.org/10.1016/0926-3373(95)00032-1